Real-Time Maximum Torque per Ampere Control of Brushless DC Motor Drive with Minimum Torque Ripple

A. Khazaee, H. Abootorabi Zarchi, and G. Arab Markadeh

***Abstract*- A nonlinear control scheme is proposed for real-time tracking of maximum torque per Ampere trajectory of the surface mounted brushless DC motor with non-sinusoidal back-EMF. The strategy employs the Lagrange's Theorem to obtain the optimum stator current, at which both torque ripple and corresponding current magnitude become minimized. A new criterion is introduced in such a way that, when forced to zero, guarantees MTPA realization. The input-output feedback linearization (IOFL) control scheme is employed to improve tracking of the applied optimum currents. In the suggested approach, the magnitude of the stator current vector is minimized effectively in each instant. The performance of the control system is validated through experimental results.**

I. Introduction

The brushless DC motor (BLDCM) have been increasingly used in various industrial and household applications, due to its high efficiency, high power density, and robust structure. In many applications, obtaining a ripple free torque control operation under minimum copper loss is the primary issue of BLDCM drives.

A wide variety of methodologies have been presented during the last two decades to minimize the torque ripple. The torque pulsation due to the commutation of the square-wave phase currents in the two-phase conduction mode has been addressed in [1, 2]. Through a comparative analysis, it has been demonstrated in [3] that the sinusoidal excited currents produce smaller torque ripple than square-wave currents. Several studies have recommended a non-sinusoidal injection scheme in which a complex Furrier series analysis is employed to determine harmonic coefficients of the reference current [4]. Both the torque ripple and copper loss minimization has been achieved by means of numerical optimization techniques [5]. In order to avoid complex exponential decomposition of these methods, Park, *et al.* [6] have proposed a straightforward solution to determine optimum current waveform using the *dq*-frame analysis, which has been previously employed for the sinusoidal permanent magnet synchronous machine (PMSM), extensively. Applying the *dq*-frame analysis to the sinusoidal PMSM, would result in constant state variables in the steady state without any position dependent terms. In the case of surface mounted PMSM, the generated torque would be a linear function of *q*-axis current. Accordingly, ripple-free torque control can be simply achieved by varying the *q*-axis current while keeping the *d*-axis current at zero. Due to non-sinusoidal back-EMF of the surface-mounted BLDCM, the *d*-axis current would appear in the torque relation which results in cross-coupling effect in torque relation. In addition, state variables would not be constant and vary with respect to the rotor angular position. In [6], in order to achieve a constant torque, the rotor position-dependent variation in the back-EMF is effectively reflected on the desired *q*-axis current, and *d*-axis current is forced to zero. Although this reference current will result in constant torque, its magnitude would not be minimum. There exist an opportunity to minimize the stator current magnitude by an MTPA strategy. It is well known that, among various control strategies, the MTPA ensures minimal copper loss [7].

In this study, a real-time MTPA strategy is proposed for BLDCM, which ensures torque ripple minimization under minimum vector current magnitude. The strategy employs Lagrange's Theorem to obtain the optimum currents. In this method a non-sinusoidal reference current, which contain fundamental and harmonic components, are developed directly without requiring complex exponential decomposition. The output torque is improved due to contribution of both fundamental and harmonic components of stator currents and back-EMFs in the torque production. The effectiveness of the proposed MTPA strategy is validated experimentally on a 200W outer rotor BLDCM prototype.

A. Khazaee and H. Abootorabi Zarchi are with Department of Engineering, Ferdowsi university of Mashhad. (Email: amir.khazaee@mail.um.ac.ir; abootorabi@um.ac.ir.

G. Arab Markadeh is with Department of Engineering, Shahrekord University. (Email: arab-gh@eng.sku.ac.ir)

II. Proposed MTPA Approach

Three-phase equivalent circuit of BLDCM drive is demonstrated in Fig. 1. The phase resistance and inductance are represented by R_s and L_s, and the phase currents and back-EMFs are demonstrated by i_j and e_j, respectively *(j=a, b, c)*. No assumption is considered on the shape of the back-EMFs; therefore, the effect of non-ideal back-EMF is considered. The electromagnetic torque T_e is given by

$$T_e = \lambda_a i_a + \lambda_b i_b + \lambda_c i_c \quad (1)$$

where λ_j is the ratio of back-EMFs with respect to the rotational speed (ω_m). The *dq*-axis variables in the rotor reference frame can be obtained by applying the power-invariant Park transformation (2) on the phase variables as

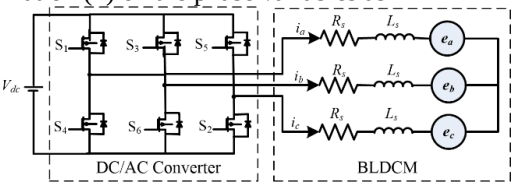

Fig. 1 Equivalent circuit of BLDCM

This article has been accepted for publication in a future issue of this journal, but has not been fully edited. Content may change prior to final publication. Citation information: DOI 10.1109/TPEL.2019.2918711, IEEE Transactions on Power Electronics

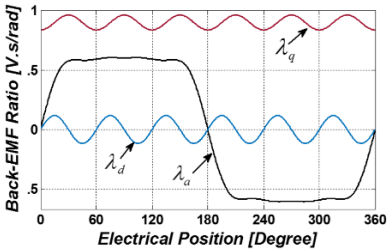

Fig. 2 Non-sinusoidal back-EMF ratio of BLDCM at rated speed

$$\begin{bmatrix} X_d \\ X_q \end{bmatrix} = \sqrt{\frac{2}{3}} \begin{bmatrix} \cos(\theta_e) & \cos(\theta_e - 2\pi/3) & \cos(\theta_e + 2\pi/3) \\ -\sin(\theta_e) & -\sin(\theta_e - 2\pi/3) & -\sin(\theta_e + 2\pi/3) \end{bmatrix} \begin{bmatrix} X_a \\ X_b \\ X_c \end{bmatrix} \quad \textbf{(2)}$$

where X is the variable and θ_e is the rotor electrical position. The electromagnetic torque and the square of the current vector magnitude can be obtained as

$$T_e = \lambda_d i_d + \lambda_q i_q \quad (3)$$

$$i^2 = i_d^2 + i_q^2. \quad (4)$$

The objective is to obtain a constant torque with minimum current magnitude. Without loss of generality, rather than the current magnitude, its square (i^2) is aimed to be minimized. In the case PMSM with sinusoidal back-EMF, λ_d is zero, and λ_q is a constant value; therefore, a constant torque can be simply achieved by controlling the q-axis current and keeping the d-axis current at zero. However, due to the non-sinusoidal back-EMF of the BLDCM, both of $\lambda_d$and λ_q would not be constant anymore and vary with respect to the electrical position as depicted in Fig. 2 for the specified motor in Table I. This results in the cross-coupling effect between the d- and q-axis currents in the torque equation.

According to (3), in order to achieve a ripple free constant torque (T_e^*), following condition must be satisfied:

$$i_q = \frac{T_e^* - \lambda_d i_d}{\lambda_q}. \quad (5)$$

In this regard, in [6], the $i_d = 0$ strategy is proposed in which the variation of back-EMF is reflected on the q-axis current as

$$i_q^* = \frac{T_e^*}{\lambda_q}, \; i_d^* = 0. \quad (6)$$

Three-phase reference currents are then deduced, using the inversed-Park transformation. Although this method is able to achieve ripple-free constant torque straightly, the current magnitude, as will be proven, would not be minimized.

According to (5), the constant torque curve can be plotted as a diagonal line with the slope of $-\lambda_d/\lambda_q$in the $i_d - i_q$ plane, as indicated in Fig. 3(a). Depending on the electrical position, the slope could be negative or positive. On the same plane, according to (4), constant current magnitude takes the form of a circle. In a particular instant ($e.g.\ \theta_e = \theta_1$), each point on the solid line produces constant torque T_e^*. Among them, the specified point (I_1^{opt}), at which the current magnitude curve becomes tangent with the torque curve will result in minimum current magnitude and hence, MTPA will be obtained. It can be obviously observed that I_0, which is the optimum point of the $i_d = 0$ strategy (6), requires greater current magnitude. In other words, in each rotor position such as $\theta_e = \theta_1$, a right-angled triangle is formed. The magnitude of the hypotenuse (I_0), is obviously greater than the magnitude of the side of

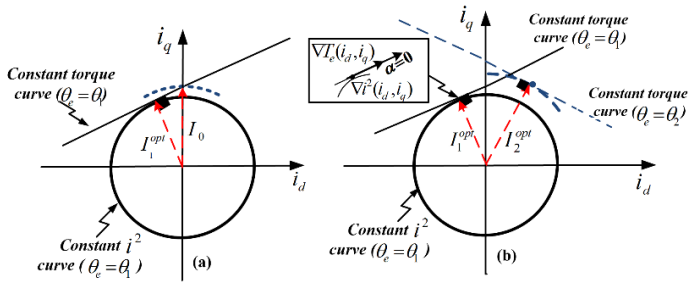

Fig. 3 Constant torque and constant current magnitude curves on the $i_d - i_q$ plane. (a): Comparison of the $i_d = 0$ and the proposed MTPA strategies. (b) Variation of the optimum point with respect to θ_e

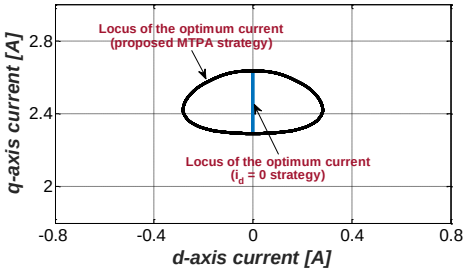

Fig. 4 Locus of the optimum point in $i_d = 0$ and the proposed MTPA strategies for the specified motor in Table I

triangle (I_1^{opt}). Therefore, rather than I_0 the control system should track I_1^{opt} to realize the MTPA strategy. Depending on the electrical position, the optimum point varies due to the variation of torque curve slope (see I_2^{opt} in Fig.3 (b)). It is observed that the optimum current vector varies with respect to the rotor electrical position. Fig.4 shows the locus of the optimum currents in both $i_d = 0$ and proposed MTPA strategies, under various electrical positions at rated speed under 2.2 Nm load. Rather than the blue curve, the control strategy should apply the black curve to the stator currents.

In order to determine the optimum conditions, according to the Lagrange's Theorem, the minimum current magnitude would be obtained at a specified point, where the current magnitude and torque curves are tangent if and only if their gradient vectors are parallel. In other words, at the point of tangency, $\Delta T_e(i_d, i_q)$ is scalar multiple of $\Delta i^2(i_d, i_q)$ as demonstrated in Fig. 3(b), and we have

$$\left\|\Delta T_e(i_d, i_q)\right\| . \left\|\Delta i^2(i_d, i_q)\right\| \sin\alpha = 0 \quad (7)$$

where α is the angle between $\Delta T_e(i_d, i_q)$ and $\Delta i^2(i_d, i_q)$. Accordingly, minimum current magnitude will be achieved when the following criterion (Γ) becomes zero:

$$\Gamma = \frac{\partial T_e}{\partial i_d}\frac{\partial i^2}{\partial i_q} - \frac{\partial T_e}{\partial i_q}\frac{\partial i^2}{\partial i_d} = 2(\lambda_d i_q - \lambda_q i_d) \quad (8)$$

In order to realize MTPA, reference currents (i_d^*, i_q^*) must be determined, such that, $\Gamma = 0$, $T_e = T_e^*$. Equating $\Gamma = 0$ yields

$$i_d^* = \frac{\lambda_d}{\lambda_q} i_q^*. \quad (9)$$

Substituting (9) in (3) results in

This article has been accepted for publication in a future issue of this journal, but has not been fully edited. Content may change prior to final publication. Citation information: DOI 10.1109/TPEL.2019.2918711, IEEE Transactions on Power Electronics

$$i_q^* = \frac{\lambda_q}{\lambda_d^2 + \lambda_q^2} T_e^* \tag{10}$$

According to (9) and (10), the *dq*-axis current references are not constant. Moreover the plant is a highly nonlinear system. Therefore, simple proportional-integral controllers may result in nonzero steady-state error, especially at higher speeds where fundamental-to-sampling frequency ratio is high. In order to cope with the tracking problem, the nonlinear IOFL control scheme is employed. The *dq*-axis currents are selected as control outputs and *dq*-axis voltages are inputs. Derivative of outputs can be obtained from dynamic model of BLDCM in the rotor reference frame [8] as follows

$$\dot{i}_d = \frac{-R_s}{L_s} i_d + \omega\, i_q - \frac{1}{L_s} e_d + \frac{1}{L_s} v_d \tag{11}$$

$$\dot{i}_q = \frac{-R_s}{L_s} i_q - \omega\, i_d - \frac{1}{L_s} e_q + \frac{1}{L_s} v_q \tag{12}$$

where ω is electrical speed. According to IOFL, the nonlinear coupled BLDCM can be transformed to an exact linear system with poles at the origin by using following control laws:

$$v_d = e_d + R_s i_d - L_s \omega\, i_q + L_s v_1 \tag{13}$$

$$v_q = e_q + R_s i_q + L_s \omega\, i_d + L_s v_2. \tag{14}$$

The decoupled closed loop system can be controlled properly by means of the proportional- integral (PI) controller as

$$\begin{bmatrix} i_d \\ i_q \end{bmatrix} = \begin{bmatrix} v_1 \\ v_2 \end{bmatrix} = \begin{bmatrix} K_p (i_d^* - i_d) + K_p/\tau_i \int (i_d^* - i_d) \cdot dt \\ K_p (i_q^* - i_q) + K_p/\tau_i \int (i_q^* - i_q) \cdot dt \end{bmatrix}. \tag{15}$$

The PI gains must be designed, such that the bandwidth set and corresponding phase margin could support fast changing variations of the reference currents in (8, 9). The block diagram of the current control loop is shown in Fig.5. According to (15), the linearized and decoupled plant is represented by an integrator. The delay introduced by sampling and algorithm execution is denoted by τ_s, which is normally equating to one switching period (τ_{sw}). Inverter assumed to have unit gain with a time constant (τ_v) equal to half of τ_{sw}. In order to actually track up to 12th harmonic, the required bandwidth should be set on $12p\omega_m^{rated}$ where p is number of pole pairs. For the specified machine in Table I, selecting $K_p = 3028$ and $\tau_i = 0.2$, would result in the required bandwidth with a phase margin equal to 64.7deg and a gain margin equal to 19.9 dB, which provide a good robustness. The block diagram of whole control system is demonstrated in Fig. 6(a).

III. Experimental Results

The effectiveness of the suggested controller is experimentally validated for a 200 W outer rotor BLDCM, characterized in Table 1. As demonstrated in Fig. 6(b), the experimental setup consists of a 200 W outer rotor BLDCM, coupled with a 250 W DC generator by a timing belt. The rotor position is sensed by means of an incremental encoder with 1024 pulses per round. Load variation can be applied by an external rheostat connected to the DC generator. A DSP-based digital control board is employed for machine drive control including the following sections. IGBT based inverter with IGBT driver, HCPL 316J, which guarantees isolation between control and power system. The inverter switching frequency is 10 kHz with the dead-time equal to 1ms. A discrete signal processor (TMS320F28335), designed with Texas Instruments Co. for motor control application. Stator phase currents and voltages are measured by three Hall-effect currents (LEM LA-55P) and voltage (LEM LV-25-P) sensors. Analog second-order low-pass filters with 2.6 kHz cut-off frequency are employed for filtering sensed currents and voltages. Internal A/D channels of DSP are used to get all measured variables.

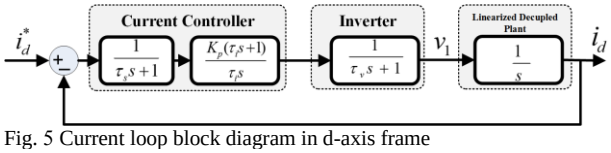

Fig. 5 Current loop block diagram in d-axis frame

A sample test has been designed to compare the performance of the proposed MTPA strategy with two other techniques. The desired torque T_e^* equal to 2.2 Nm (33% of rated) is experimentally applied to three control methodologies. In the first method, sinusoidal (constant *dq*-axis) currents are applied to the stator to provide the demanded torque. In the second method, the $i_d = 0$ strategy [6], and in the third one, the proposed MTPA strategy is applied to the control system. Results are presented in Fig. 7. In Figs. 7 (a), (b) the experimental results of the sinusoidal current injection scheme are demonstrated. The *q*-axis current is controlled at its desired constant value, while the *d*-axis current is kept constant at zero.

TABLE I MACHINE PARAMETERS

Rated speed	30 *rad/s*
Rated torque	6.6 *Nm*
Number of pole pairs	8
R_s, L_s	0.56Ω, 1.24 *mH*

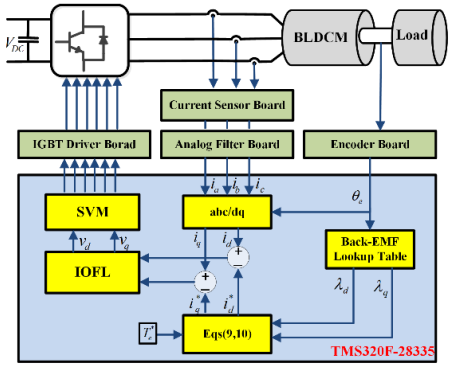

(a)

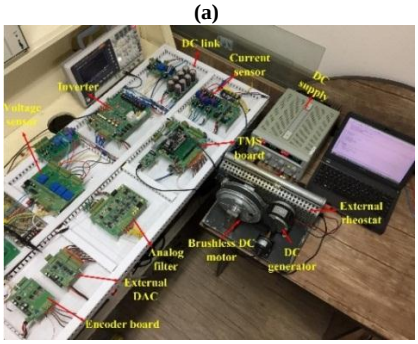

(b)

Fig. 6 (a) Diagram of the proposed MTPA strategy (b) Experimental setup

This article has been accepted for publication in a future issue of this journal, but has not been fully edited. Content may change prior to final publication. Citation information: DOI 10.1109/TPEL.2019.2918711, IEEE Transactions on Power Electronics

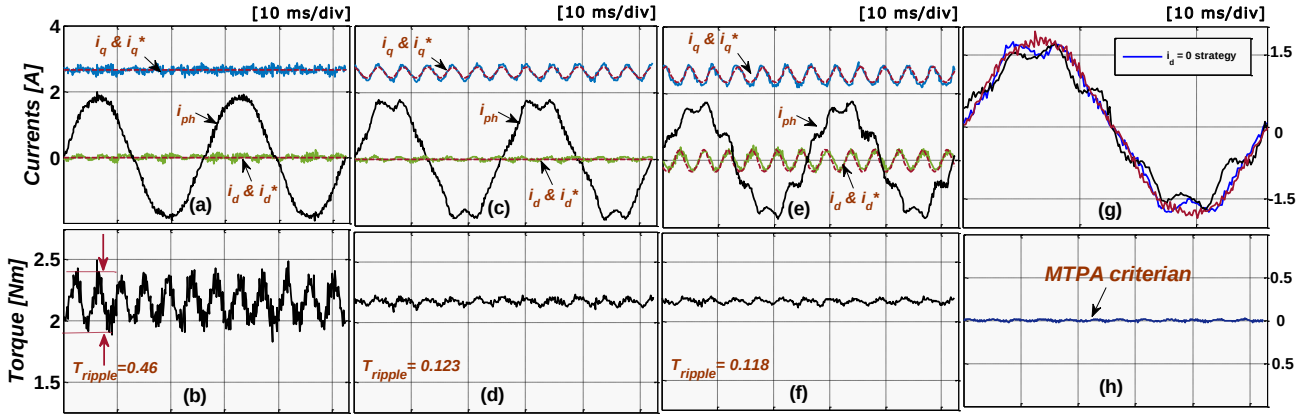

Fig.7 Experimental results of applying (a), (b): sinusoidal current injection scheme, (c), (d) the $i_d = 0$ strategy, (e), (f): Proposed MTPA strategy, (g): comparison of phase currents, and (h): MTPA criterion in the proposed MTPA.

It can be seen that undesirable torque ripples are generated; however, these ripples are much less than the square-wave current injection scheme [3].

Torque ripple is reduced significantly in the second method (Figs. 7(c), (d)), in which the back-EMF variations are being reflected on the *q*-axis current while keeping the *d*-axis current at zero (6). However, as demonstrated earlier there exist an opportunity to reduce the required current magnitude to provide the same load torque by the proposed MTPA strategy. It is obviously observed in Figs. 7 (e), (f), that the variations of the back-EMF are reflected on both *d*- and *q*-axis current references to achieve both torque ripple reduction and current magnitude minimization, simultaneously. In addition, current controller has succeeded to track its desired value. The MTPA criterion is forced to zero as shown in Fig.7 (h). All three phase currents are indicated in the Fig.7 (g). As demonstrated, in comparison with $i_d = 0$ strategy, the realization of the proposed MTPA has effectively reduced the current magnitude at each instant under the same load conditions. Peak-to-peak value of torque ripple (T_{ripple}) in each method is also presented in Fig.7.

In order to analyze how the suggested method improves the torque production, exponential decomposition of back-EMFs and currents are employed as following

$$\lambda_a = \lambda_1 \sin\omega t + \lambda_3 \sin 3\omega t + \lambda_5 \sin 5\omega t + \lambda_7 \sin 7\omega t \qquad (16)$$

$$i_a = I_1 \sin\omega t + I_5 \sin 5\omega t + + \lambda_7 \sin 7\omega t \qquad (17)$$

Third harmonic of stator current would not be circulated due to Y connection of windings. Regarding (1), interaction of currents and back-EMFs produce following torque profile[9].

$$T = T_0 + T_6 \cos 6\omega t + T_{12} \cos 12\omega t \qquad (18)$$

$$T_0 = \left[\lambda_1 I_1 + \lambda_5 I_5 + \lambda_7 I_7\right], \quad T_6 = \left[(\lambda_7 - \lambda_5) I_1 - \lambda_1 I_5 + \lambda_1 I_7\right], \quad T_{12} = \left[-\lambda_7 I_5 - \lambda_5 I_7\right]$$

In the sinusoidal current injection scheme (I_5=I_7=0), it is the fundamental components of the currents and back-EMFs that contribute in the torque production. In the non-sinusoidal harmonic injection scheme (NSHI), injected current harmonics are determined to minimize torque ripple by eliminating T_6 and T_{12}. Moreover, dc component (T_0) increases due to contribution of both fundamental and harmonic components in torque production. In comparison with (NSHI) [4], the suggested approach has two improvements:

- Rather than complex exponential decomposition, the optimum reference current in the proposed method would be obtained simply by forcing the MTPA criterion to zero.
- Unlike NSHI strategy, in which limited harmonic components are considered to reduce complexity, the proposed one considers all harmonic components since it considers general form of back-EMF.

The harmonic components of injected stator currents for each method of Fig.7 is demonstrated in Fig.8 (a). As demonstrated in Fig.8 (b), 6th component and its coefficients are appeared in the produced torque. The harmonic components of produced torque is reduced in both $i_d = 0$ and the proposed MTPA strategies by automatically injecting current harmonics. In comparison with $i_d = 0$ strategy, the reference current harmonics in the proposed MTPA are determined such that RMS value of current is minimized. The ratio of average torque per Ampere (RMS) (T/I) is demonstrated for each method in Fig.8 (c). Increment of this parameter in the proposed method implies that as per a constant current, the produced torque has been increased in this method. This occurs due to contribution of both fundamental and harmonic components of the currents and back-EMFs in the torque production.

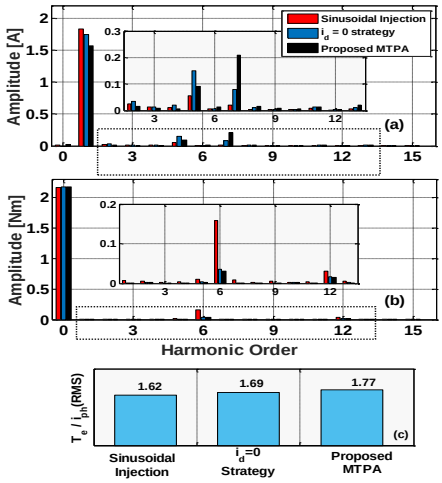

Fig.8 (a) FFT of phase current, (b) FFT of produced torque, (c) ratio of average torque per Ampere

This article has been accepted for publication in a future issue of this journal, but has not been fully edited. Content may change prior to final publication. Citation information: DOI 10.1109/TPEL.2019.2918711, IEEE Transactions on Power Electronics

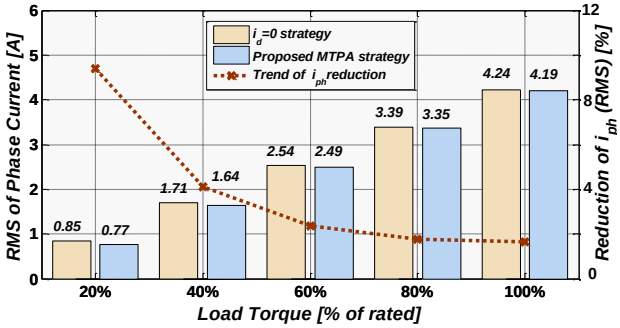

Fig.9 Comparison of the RMS value of phase current in the $i_d = 0$ and the proposed MTPA strategy

The performance of the proposed MTPA strategy in various load conditions is demonstrated in Fig. 9. The RSMS value of the phase current i_{ph} is compared for $i_d = 0$ and the proposed MTPA strategies in different load conditions. The trend of reduction in RMS value of i_{ph}, is denoted by the dotted curve. The RMS of phase current, required to produce same torque, is indicated to have 1.5% to 9% reduction depending on load torque, in such a way that, the rate of reduction is more dominant at light loading conditions.

In order to illustrate torque control performance, a step change in torque command from 3.5 Nm to 4.5 Nm is applied to the proposed control approach of Fig.6 (a) at 2.5s. The response of torque and corresponding *dq*-axis currents are demonstrated for rotational speed equal to 10 rad/s in Fig.10 (a), (b) and for speed of 30 rad/s in Fig.10 (c), (d). It is clearly observed that the back-EMF variations are reflected on both *d*- and *q*- axis currents to obtain the desired torque with minimum ripples as per the minimum current. Consequently, torque is properly tracked at its commanded value while the MTPA criterion is forced to zero to guarantee MTPA realization.

Fig.11 shows performance of the proposed MTPA in comparison with sinusoidal injection under different loading conditions equal to 2.2, 4.4 and 6.6 Nm. The produced torque and corresponding MTPA criterion in each load is presented in Fig.11 (a) and Fig.11 (b), respectively. When MTPA is applied, torque ripple is reduced effectively and MTPA criterion is forced to zero, that guarantees minimum copper loss.

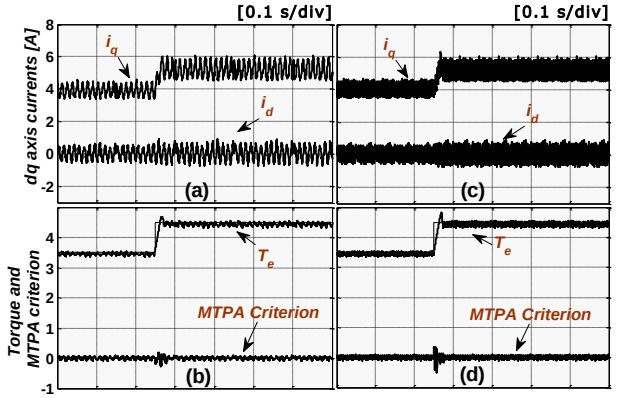

Fig.10: Response of proposed MTPA to a step change in torque reference and corresponding dq-axis currents at (a), (b): 10 rad/s and (c), (d) 30 rad/s

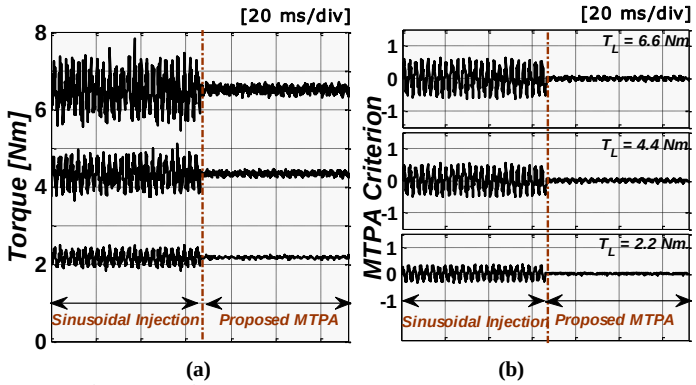

Fig.11: Performance of the proposed MTPA in comparison with sinusoidal injection scheme under load torque equal to 2.2, 4.4 and 6.6 Nm at 20 rad/s (a): load torque, and (b) MTPA criterion

IV. Conclusions

A new MTPA control strategy based on Lagrange's Theorem has been developed and validated for BLDCM. The optimized *dq*-frame current waveforms of the proposed MTPA are applied as the reference values and the motor winding currents are forced to track them employing the IOFL method. Both analytical study and experimental results have revealed that applying the proposed MTPA strategy would result in both torque ripple and current magnitude minimizations simultaneously, especially under light loading conditions.

References

[1] W. Jiang, H. Huang, J. Wang, Y. Gao, and L. Wang, "Commutation Analysis of Brushless DC Motor and Reducing Commutation Torque Ripple in the Two-Phase Stationary Frame," *IEEE Transactions on Power Electronics*, vol. 32, pp. 4675-4682, 2017.

[2] H. Lu, L. Zhang, and W. Qu, "A New Torque Control Method for Torque Ripple Minimization of BLDC Motors With Un-Ideal Back EMF," *IEEE Transactions on Power Electronics*, vol. 23, pp. 950-958, 2008.

[3] M. Bertoluzzo, G. Buja, R. K. Keshri, and R. Menis, "Sinusoidal Versus Square-Wave Current Supply of PM Brushless DC Drives: A Convenience Analysis," *IEEE Transactions on Industrial Electronics*, vol. 62, pp. 7339-7349, 2015.

[4] P. Kshirsagar and R. Krishnan, "High-Efficiency Current Excitation Strategy for Variable-Speed Nonsinusoidal Back-EMF PMSM Machines," *IEEE Transactions on Industry Applications*, vol. 48, pp. 1875-1889, 2012.

[5] F. Aghili, M. Buehler, and J. M. Hollerbach, "Experimental characterization and quadratic programming-based control of brushless-motors," *IEEE Transactions on Control Systems Technology*, vol. 11, pp. 139-146, 2003.

[6] P. Sung Jun, P. Han Woong, L. Man Hyung, and F. Harashima, "A new approach for minimum-torque-ripple maximum-efficiency control of BLDC motor," *IEEE Transactions on Industrial Electronics*, vol. 47, pp. 109-114, 2000.

[7] C. Lai, G. Feng, J. Tjong, and N. C. Kar, "Direct Calculation of Maximum-Torque-Per-Ampere Angle for Interior PMSM Control Using Measured Speed Harmonic," *IEEE Transactions on Power Electronics*, vol. 33, pp. 9744-9752, 2018.

[8] A. Khazaee, H. Abootorabi Zarchi, and G. Arab Markadeh, "Loss model based efficiency optimized control of brushless DC motor drive," *ISA Transactions*, vol. 86, pp. 238-248, 2019/03/01/ 2019.

[9] M. Shirvani Boroujeni, G. R. A. Markadeh, and J. Soltani, "Torque ripple reduction of brushless DC motor based on adaptive input-output feedback linearization," *ISA Transactions*, vol. 70, pp. 502-511, 2017/09/01/ 2017.